https://doi.org/10.5194/egusphere-2022-208
Preprint. Discussion started: 11 May 2022

A theory of abrupt climate changes: their genesis and anatomy

Hsien-Wang Ou[1]
[1] Lamont-Doherty Earth Observatory, Columbia University, Palisades, NY10964, USA
Corresponding author: Hsien-Wang Ou (hsienou0905@gmail.com)

Abstract. We integrate our previous ice-sheet and climate models to examine abrupt climate changes pertaining to Heinrich event (HE), Dansgaard-Oeschger (DO) cycle as well as last deglaciation punctuated by Younger Dryas (YD). Since they are all accompanied by ice-rafted debris, we posit their common origin in the calving of ice sheet due to thermal switch at its bed. Such thermal switch would generate step-like freshwater flux and together with decadal ocean response, they would endow abruptness to these millennial climate signals, which need not involve ocean mode change, as commonly assumed. We distinguish thermal switches due to geothermal heat and surface melt, which would calve inland/marginal ice to drive HE/DO-cycle, respectively. As such, the glacial DO-cycle hinges on post-HE warmth that enables the ablation whereas the Holocene DO-cycle is self-sustaining. The ocean response to freshwater flux entails millennial adjustment to maximum entropy production (MEP), a process termed "MEP adjustment". As its direct consequence, the termination of HE is accompanied by sudden warming followed by gradual cooling to exhibit saw-toothed H-cycle, and the cooling moreover would anchor DO-cycles to form the hierarchical Bond cycle. The meltwater produced during deglaciation, if rerouted to Hudson Bay, may augment the calving-induced freshwater flux to cause YD, the latter thus involves happenstance and did not materialize during penultimate deglaciation. By incorporating calving origin of the freshwater flux and MEP adjustment of the ocean, the theory has provided an integral account of these abrupt climate changes.

Non-technical summary

We integrate our previous models to examine abrupt climate changes pertaining to Heinrich and Dansgaard-Oeschger cycles as well as deglaciation punctuated by Younger Dryas. We posit their common origin in the calving of ice sheet triggered by thermal switches at its bed, which are differentiated between that caused by geothermal heat and surface melt. Together with the ocean evolution toward maximum entropy production, the theory provides an integrated account of observed phenomena.

1. Introduction

Last ice age was teemed with abrupt climate changes pertaining to Heinrich (H) events (HE), Dansgaard-Oeschger (DO) cycles as well as deglaciation punctuated by Younger Dryas (YD), a dramatic climate reversal. While these climate signals are distinct, they are all accompanied by ice-rafted debris (IRD, Bond et al. 1997, Fig. 6), suggesting a common origin in the calving of ice sheet due to thermal switch at its bed (MacAyeal 1993; Ou 2022a). Since recurring time of calving is constrained by ice mass balance, the resulting freshwater flux is naturally availed the millennial timescale, a timescale not inherent to the ocean. On the other hand, thermal switch is

https://doi.org/10.5194/egusphere-2022-208
Preprint. Discussion started: 11 May 2022

operating on very short (years) subglacial hydrological timescale (Fricker et al. 2007) to render step-like freshwater flux, and together with the decadal ocean response (Duplessy et al. 1991), they endow abruptness to the millennial climate signal, which thus need not involve mode change, as commonly assumed (Alley et al. 2003). Besides the abruptness, the presumed mode change is also prompted by large signal in the surface-air temperature (SAT), which however may simply reflect extremely cold winter air during stadials characterized by extensive sea-ice cover (Denton et al. 2005) whereas variation in the sea-surface temperature (SST) remains well short of mode change except during deglaciation (Bard 2002).

With above common origin in the thermal switch at the ice bed, we nonetheless distinguish their two differing heat sources hence locales: for H-cycle, it is the trapping of the geothermal heat by the growing ice sheet that leads to calving of the inland ice (MacAyeal 1993); and for DO-cycle, it is the surface melt over the ablation zone (Hooke 1977) that causes calving of the marginal ice. Both these thermal switches hence differing calving processes have been demonstrated by numerical calculations (Calov et al. 2002; Brinkerhoff and Johnson 2015), and our ice-sheet model (Ou 2022a) allows a prognosis of the resulting freshwater flux, which thus may be prescribed as external perturbation of the ocean.

To examine the ocean response, we shall apply our box model of coupled ocean/atmosphere (Ou 2018). As deduced therein, since the meridional overturning circulation (MOC) involves random eddy exchange across the subtropical front, a generalized second law of nonequilibrium thermodynamics (NT) leads to its millennial evolution toward maximum entropy production (MEP), a process termed "MEP adjustment". Incorporating this process, Ou (2022b, under review) has examined the ocean response to the orbital forcing and shows that it can reproduce Pleistocene glacial cycles while resolving many longstanding puzzles, in support of its utility. In the present theory, we shall show that combining calving of the ice sheet and MEP adjustment of the ocean, it may provide an integrated account of abrupt climate changes.

For self-containment, we first discuss in Sects. 2 and 3 the relevant physics of our ice-sheet and climate models, respectively, which is then applied in Sects. 4 to 6 to examine successively abrupt climate changes pertaining to H- and DO-cycle as well as deglaciation. In each, we highlight salient features of the observed phenomena, discuss their genesis based on model physics, and provide a synthesis of previous works. We summarize main findings of the theory in Sect. 7 to conclude the paper.

2. Ice-sheet model

We first discuss our ice-sheet model (Ou 2022a), which provides the freshwater perturbation to the ocean. It is well recognized that large ice sheet may exhibit quasi-periodical surge due to thermal switch at its bed (MacAyeal 1993). Physically, ice growth by accumulation would increasingly trap the geothermal heat to warm the bed to the pressure-melting point when a surge is triggered; the ensuing thinning would augment the conductive cooling to refreeze the bed, terminating the surge. As the thermal switch is also favored by greater driving stress, it would be sited

https://doi.org/10.5194/egusphere-2022-208
Preprint. Discussion started: 11 May 2022

off the ice divide to calve inland ice through Hudson Strait, which has been widely attributed as the source of H-events (Bond et al. 1992). The numerical simulation of the ice discharge however often involves tuning of the sliding velocity (Calov et al. 2002), which directly impacts the amplitude and period of the surge cycle. To remove this empiricism, we have incorporated global momentum balance to constrain the sliding velocity by the strait width (Tulaczyk et al. 2000), so the model closure allows us to prognose the surge properties.

A tangible outcome of the model is the construction of a 2-D regime diagram as sketched in Fig. 1, which is spanned by scaled length (l) and width (w) of the ice discharge and on which surge properties, such as termination height (h), surge/creep duration (t_s/t_c), and surge velocity (u), can be contoured (all nondimensionalized). It is seen that the model has delineated three dynamical regimes: steady creep, steady sliding and cyclic surge separated by thick and shaded lines, which can be understood as follows. For short discharge, the catchment due to accumulation can be absorbed by creep to maintain a steady state, so the thermal switch remains off. For longer discharge, the thermal switch would turn on to trigger the sliding motion whose strength however depends on the strait width: for a narrower strait hence slower sliding, the ice flux can be sustained by catchment to maintain a steady state, but for a wider strait hence faster sliding, the ice flux cannot be sustained, thus vaulting into surge cycle. The box marked H represents ice discharge through the Hudson Strait, which falls well within the surge regime, and the prognosed surge properties are of the same order as that inferred from observation, in support of ice-calving source of the H-cycle.

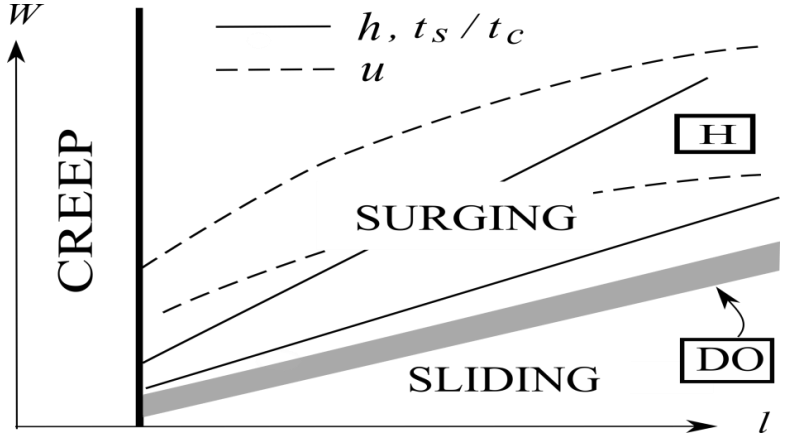

Fig. 1. A schematic of the regime diagram spanned by the scaled length l and width w of the ice discharge, which consists of steady-creep, steady-sliding and cyclic-surge regimes separated by thick and shaded lines. Contoured surge properties (thin lines) include termination height (h), surge/creep duration (t_s/t_c), and surge velocity (u). Box H marks the ice discharge through Hudson Strait, and the shaded line indicates its aspect ratio for the DO-cycle.

https://doi.org/10.5194/egusphere-2022-208
Preprint. Discussion started: 11 May 2022

Since DO-cycle is associated with much smaller freshwater flux than H-cycle, it likely involves calving of the marginal ice. Searching for clues that might differentiate the two, we note that englacial ice-sheet temperature shows two distinct zones of temperate bed (Hooke 1977, Fig. 4d): besides the one under ice divide due to trapping of the geothermal heat, there is another one in the ablation zone where surface melt is particularly effective in warming the bed via vertical advection. We posit therefore that DO-cycle is driven by the thermal switch under the ablation zone, which would calve the marginal ice. Unlike ice discharge through Hudson Strait, this calving may occur along the eastern seaboard of Laurentide ice sheet (LIS) hence unconstrained by topography, and numerical calculations of ice discharge over a flatbed (Brinkerhoff and Johnson 2015) provides an apt demonstration of its plausible scenario: following the thermal trigger, the surging ice would grow in width until it is arrested by a limit cycle, resulting in periodic self-organized ice streams.

Since the thermal switch underlying Fig. 1 is generic, the stream width arrested by limit cycle is precisely that divides the steady-sliding and cyclic-surge regimes (shaded). Denoting the corresponding stream properties by subscript "s", they are functions only of the "heating" parameter measuring the relative strength of the frictional to geothermal heating

$$\alpha_h = \rho_i g \dot{a}[h]/\dot{g} \tag{1}$$

where ρ_i is the ice density, g, the gravitational acceleration, $\dot{a}$, the accumulation, $[h]$, the ice thickness scale taken to be equilibrium-line altitude (ELA), and $\dot{g}$, the geothermal flux. Specifically, the termination height is

$$h_s = (\sqrt{1 + 2\alpha_h} - 1)/\alpha_h, \tag{2}$$

the aspect ratio is

$$a_s = \sqrt{2}/h_s, \tag{3}$$

and the ratio of surge/creep durations is

$$t_{ratio} = 2(1 - a_s^2)^{-1} \tag{4}$$

for which we have set the mean thinning rate of the surge to be half its maximum. They are plotted in Fig. 2 whose qualitative dependence can be explained as follows: for stronger frictional heating, the ice would be thinner before the conductive cooling may terminate the surge, which in turn would be wider on account of the mass balance, and then such wider surge implies faster sliding motion to shorten the surge relative to the creep phases. Applying standard values listed in Appendix, the heating parameter is .48 (dashed), which yields a fractional surface depression of .17, quite smaller than that of HE (about .5, see Ou 2022a). The surge and creep have compa-

https://doi.org/10.5194/egusphere-2022-208
Preprint. Discussion started: 11 May 2022

rable duration ($t_{ratio} = 1.1$), both lasting about 1 ky. In comparison with the saw-toothed H-cycle, the shorter creep is due to the smaller surface depression during surge, which needs less time to be replenished by accumulation, but the surge duration is maintained by the slower discharge hence thinning.

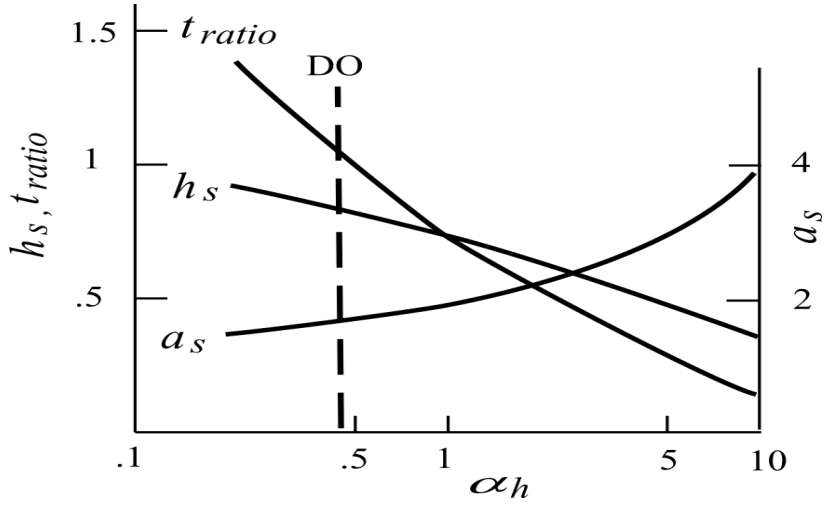

Figure 2: Ice-discharge properties of the DO-cycle plotted against the heating parameter. They are the termination height h_s, aspect ratio a_s and ratio of surge/creep durations t_{ratio}, all nondimensionalized. The vertical dashed line is representative of the DO-cycle, which shows comparable surge/creep durations.

To recap, our ice-sheet model has produced surge properties required by H- and DO-cycles, so the resulting freshwater flux may be prescribed as external to the ocean to examine its response, as discussed next.

3. Climate model

Readers are referred to Ou (2018) for detailed derivation of our coupled climate model, only relevant physics is summarized here for self-containment. The model configuration is sketched in Fig. 3 for which both planetary fluids are composed of warm/cold boxes aligned at mid-latitudes and the adjacent ice sheet injects freshwater perturbation into the subpolar water, as determined from our ice-sheet model. Retaining dominant balances, the absorbed SW flux (q) differentiates the SST (T), which differentiates the SAT by the convective flux (q_c) to induce atmospheric heat transport; the attendant moisture transport depresses the subpolar salinity (S), which together with the SST specifies the density surplus (ρ); the latter drives the MOC (K) across the subtropical front composed partly of random eddy shedding. Since climate signals of our concern are

https://doi.org/10.5194/egusphere-2022-208
Preprint. Discussion started: 11 May 2022

158 dominated by that of the cold-box, the model variables are the nondimensionalized cold-box de-
159 viations from (known) global means.

160

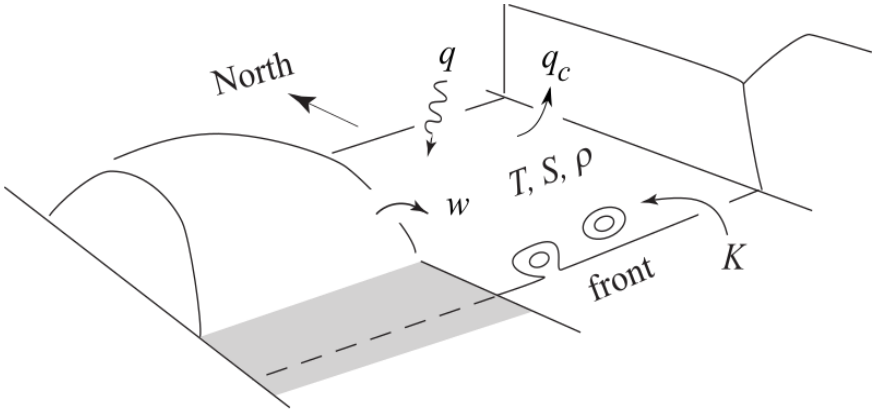

161

162 **Figure 3:** The model configuration of coupled ocean/atmosphere composed of warm and
163 cold boxes aligned at mi-latitudes and ice sheet on the adjacent continent providing fresh-
164 water perturbation to the subpolar ocean. Model variables are the cold-box deviations
165 from (known) global means and the MOC.

166 The model physics can be illustrated via a phase-space diagram sketched in Fig. 4 whereby the
167 cold-box temperature deficit (T) and density surplus (ρ) are plotted against MOC (K). Expect-
168 edly, decreasing MOC cools the subpolar water (that is, increasing temperature deficit) and re-
169 duces the convective flux from its global mean ($\bar{q}_c$), but since the convective flux may not be
170 negative, the ocean/atmosphere coupling renders a "convective bound" at

171 $$T = T_c \equiv 2\bar{q}_c \,, \qquad (5)$$

172 which divides the climate regime into warm/cold branches with a break in the density slope.
173 Since the cold branch is characterized by vanishing convective flux, the atmospheric heat
174 transport is saturated at $\bar{q}_c$. This division into warm/cold branches is an outcome of atmospheric
175 coupling, which unlike ocean-only models (Stommel 1961) allows normal-signed density con-
176 trast, as seen in coupled climate models (Rahmstorf et al. 2005). That the cold branch is charac-
177 terized by vanishing convective flux is consistent with diagnosis of the cold state from such
178 models (Manabe and Stouffer 1988, their Fig. 18), in support of the convective bound.

179

https://doi.org/10.5194/egusphere-2022-208
Preprint. Discussion started: 11 May 2022

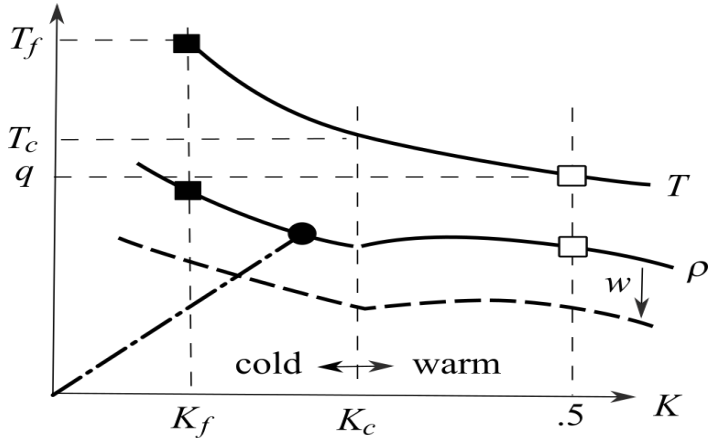

Figure 4: A schematic of the regime diagram whereby subpolar temperature deficit (*T*) and density surplus (ρ) are plotted against MOC (*K*). The convective bound (subscripted *c*) separates warm/cold branches with their respective MEP (rectangles). The glacial MEP (solid rectangles) is defined by the freezing-point (subscripted *f*) subpolar temperature. The MOC line (dash-dotted) pivots on millennial timescale toward MEP, whose intersect with the density curve specifies the ocean state (oval). The density curve is displaced (thick-dashed) instantaneously by the freshwater flux (*w*).

To constrain MOC, we assume it to be proportional to the density surplus (Stommel 1961), as indicated by dash-dotted line (referred as "MOC line") whose intersect with the density curve then specifies the climate state (oval). In numerical models that do not resolve eddies, the MOC line is fixed by diapycnal diffusivity, which in effect is a free parameter finely tuned to yield the observed state (Rahmstorf et al. 2005), but the actual MOC is subjected to random eddy exchange across the subtropical front (Auer 1987; Lozier 2010) and applying the fluctuation theorem --- a generalized second law (Crooks 1999), we deduce that the MOC line would pivot on millennial timescale toward MEP, a process termed "MEP adjustment". There can be MEP in both warm/cold branches, which are referred as interglacial (open rectangles) and glacial (solid rectangles) MEPs, respectively.

The interglacial MEP is derived to be $(T, K = q, 1/2)$, which is consistent with the observed interglacial; and the glacial MEP is specified by freezing-point subpolar water $(T = T_f)$ that is free of perennial ice. The reason for the latter is because such ice would curb the ocean cooling to weaken the MOC --- in contradiction to MEP. This glacial MEP is consistent with that observed during last glacial maximum (LGM) characterized by freezing-point subpolar water (Kucera et al. 2005), which remains open in summer (de Vernal et al. 2005). Since MEP adjustment operates on millennial timescale, the above deduction does not preclude perennial sea ice during abrupt climate change, and then with SST being at the freezing point, extensive sea ice necessarily forms in winter, both as seen later.

https://doi.org/10.5194/egusphere-2022-208
Preprint. Discussion started: 11 May 2022

The freshwater flux from the calving ice would depress the density curve as indicated by an arrow toward the dashed line. The displacement of the density curve is assumed instantaneous relative to the millennial climate signals (Sect. 1). On the other hand, the orbital forcing hence the temperature curve may be taken as unvarying through abrupt climate changes.

4. H-cycle

4.1 Phenomenology

The last glacial was punctuated by recurring Heinrich events (HE) when massive calving of icebergs strewed IRD across the North Atlantic (Heinrich 1988; Bond et al. 1992). As discussed in Sect. 1, the onset and termination of HEs are abrupt relative to their millennial duration spaced several millennia apart (Elliot et al. 2002). The accompanying freshwater flux is substantial, amounting to sea-level change of O (10 m) (Chappell 2002), which further depresses MOC from its already weak glacial strength (Elliot et al. 2002). Since the subpolar water is already at the freezing point (Kucera et al. 2005), a weakening of MOC causes formation of extensive sea ice to maintain the ocean heat balance (Broecker 1994). The ice-covered ocean deters melting of icebergs, allowing IRD to spread to the glacial polar front (Grousset et al. 1993; van Kreveld et al. 2000).

The MOC resumes at the termination of HE, the subpolar water however does not merely return to the pre-HE state of freezing-point temperature, but a state several degrees warmer (Bard 2002). This post-HE warming is followed by gradual cooling to the pre-HE glacial state, thus forming the saw-toothed H-cycle (Alley 1998; Henry et al. 2016) --- albeit the cooling trend is populated by millennial DO-cycles. While SAT signal associated with H-cycle spans O (10 ^{0}C), the SST variation is considerably smaller, ranging in low single digits (Alley 1998; Bard 2002). The substantial change in MOC has led to anti-phased Antarctic climate during HE, outside of which the hemispheric climates remain synchronous (Broecker 1998; Clark et al. 1999).

4.2 Genesis

As discussed in our ice-sheet model, we posit HE to originate from calving of the inland ice through Hudson Strait. We illustrate the ocean response to the freshwater flux via a phase-space diagram in Fig. 5 with the resulting timeseries shown in Fig. 6. As a representative example, we set the annual absorbed SW flux at 90 $W\ m^{-2}$ below the global mean, global convective flux at 56 $W\ m^{-2}$, global-mean SST at 14 ^{0}C and anomalous freshwater flux at .1 *Sv*, so for scales defined in Appendix, they yield dimensionless parameters $\left(q, \bar{q}_c, T_f, w\right) = (0.9, 0.56, 1.75, 0.05)$; and for the time series, we set the surge/creep duration at 1/5 ky with light/dark shades symbolizing freshwater flux and sea-ice cover, respectively.

https://doi.org/10.5194/egusphere-2022-208
Preprint. Discussion started: 11 May 2022

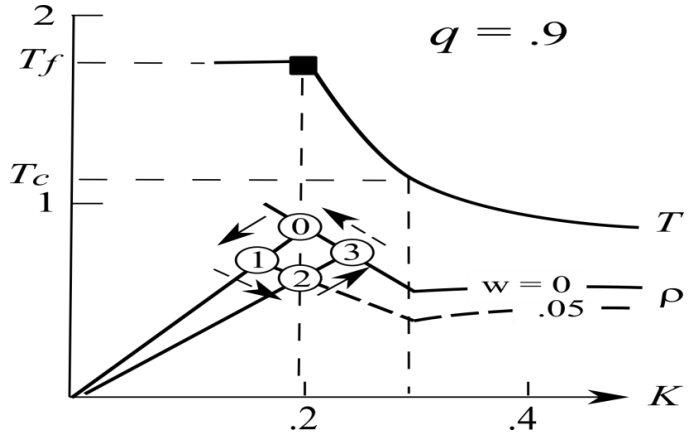

240

241 **Figure 5:** The H-cycle in the phase-space diagram when the freshwater flux displaces
242 the density curve (thick dashed). The cycle goes through numbered states with solid ar-
243 rows indicating abrupt changes and dashed arrows, the millennial adjustment to MEP
244 (solid rectangle).

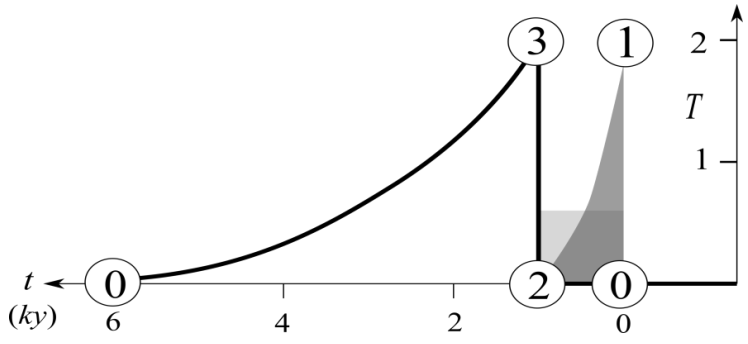

245

246 **Figure 6:** A schematic of H-cycle in the time domain corresponding to that of Fig. 5.
247 Light and dark shades symbolize freshwater flux and sea-ice extent, respectively.

248 The H-cycle begins with the glacial MEP (State 0) when the thermal switch is turned on and runs
249 through numbered states with solid and dashed arrows indicating fast (decadal) and slow (millen-
250 nial) transits, respectively. Since the MOC line pivots on millennial timescale, it remains immo-
251 bile at the HE onset, so State 0 would transition to State 1 whereby the weaker MOC would in-
252 duce extensive sea ice (dark-shaded in the time plot) to maintain the ocean heat balance. During
253 the millennial HE, the MOC line would pivot toward MEP by melting the sea ice (Sect. 3) hence
254 transition State 1 to 2. At the HE termination, the MOC line is again immobile to transition State
255 2 to 3, which thus exhibits a sudden warming. During the ensuing creep phase, the MEP adjust-
256 ment would pivot the MOC line toward the glacial MEP (State 0), thus evincing a gradual cool-
257 ing to form the saw-toothed H-cycle.

https://doi.org/10.5194/egusphere-2022-208
Preprint. Discussion started: 11 May 2022

A key property of the H-cycle is the post-HE warmth, which can be derived as follows. As the H-cycle resides in the cold branch for which the atmospheric heat transport has saturated at the global convective flux $\bar{q}_c$ (Sect. 3), the total heat transport (given by the orbital forcing q) is partitioned between atmosphere and ocean as

$$q = \bar{q}_c + KT \,, \tag{6}$$

and the salinity balance states

$$\mu\bar{q}_c + w = KS \tag{7}$$

where μ is a moisture parameter so the first term is the atmospheric moisture transport, which together with the freshwater flux w is balanced by the salinity flux carried by MOC. Combining these two equations yields the density surplus

$$\rho = T - S \tag{8}$$

$$= \frac{1}{K}(q_e - w) \,, \tag{9}$$

where

$$q_e = q - (1+\mu)\bar{q}_c \tag{10}$$

is the forcing in excess of the warm-transition threshold (the last term), the latter being the maximum insolation (that is, $w = 0$) when the ocean may stay in the cold branch (that is, $\rho \geq 0$). From Eqs. (6), (9) and trigonometry, we derive that

$$\frac{T_3}{T_2} = \frac{K_2}{K_3} \tag{11}$$

$$= \frac{\rho_2}{\rho_3} \tag{12}$$

$$= \frac{K_3}{K_2} \cdot \frac{q_e - w}{q_e} \,, \tag{13}$$

so Eqs. (11) and (13) yield

$$\frac{K_2}{K_3} = \left(1 - \frac{w}{q_e}\right)^{1/2} . \tag{14}$$

Substituting Eqs. (14) into (11), we arrive at

https://doi.org/10.5194/egusphere-2022-208
Preprint. Discussion started: 11 May 2022

$$\frac{T_3}{T_2} = (1 - \frac{w}{q_e})^{1/2} \quad (15)$$

The (dimensional) temperature range (ΔT) of the H-cycle thus is

$$\Delta T = [T](T_2 - T_3)$$

$$\approx \bar{T} \cdot \frac{w}{2\, q_e}\,, \quad (16)$$

for which we have assumed $w/q_e \ll 1$. For parameter values specified earlier, $q_e = .17$, so $w/q_e = .29$, the approximation Eq. (16) thus yields $\Delta T \approx 2\ ^0$C (as shown in Fig. 6), which represents an underestimate of about 10 %. Given crudeness of the model, we prognose therefore a post-HE warmth in low single digits, which is commensurate with the observed one (Bard 2002). Since this warmth increases with the freshwater flux and summer insolation, it would lead to deglaciation when certain threshold is exceeded, a topic to be discussed in Sect. 6.

4.3 Synthesis

The post-HE warming has been attributed to resumption of MOC, which however does not merely return the subpolar water to the pre-HE state but a few degrees warmer, and the subsequent cooling has been ascribed to the downwind effect of growing LIS during the binge phase (Alley 1998), whose efficacy remains to be demonstrated (Clark 1992). In our interpretation, on the other hand, both these features are direct consequences of the MEP adjustment: by melting sea ice during HE, it flattens the MOC line, which necessarily yields a warmer state at the termination of HE; then the same process would cool the subpolar water toward the glacial MEP defined by freezing point; there is no need to invoke disparate or extraneous physics.

With the gradual cooling being the climate response to HE, it does not precondition HE (Alley and Clark 1999), which runs on the internal ice clock (Sect. 2). On the other hand, the climate response to the primary ice calving through Hudson Strait would synchronize calving of lesser ice sheets around the North Atlantic to augment the freshwater flux (Grousset et al. 1993). The sea-ice cover during HE is induced by MOC weakened by freshening, so it is a continuous function of the freshwater flux, which moreover is dissipating through HE; a distinct H-mode from the glacial state thus cannot be defined nor is it necessary (Alley and Clark 1999).

Because of abruptness of the post-H warming and the large annual SAT signal registered in the ice core, H-cycle has been modelled as ocean mode change (Paillard 1995; Ganopolski and Rahmstorf 2001), which is unsupported by observation: the abruptness merely reflects the decadal ocean response to step-like freshwater perturbation (Sect. 1) and the large SAT signal stems from the extremely cold winter air during HE due to extensive sea ice cover (Broecker 1994; Li et al. 2010). In contrast to SAT, the SST signal ranges only in low single digits (Bard 2002) and is proportional to the freshwater perturbation Eq. (16), both negating their interpretation as mode

https://doi.org/10.5194/egusphere-2022-208
Preprint. Discussion started: 11 May 2022

change. While short of mode change, the abrupt MOC change associated with HE is nonetheless of sufficient magnitude (Elliot et al. 2002) to induce anti-phased Antarctic climate (Broecker 1998; Clark et al. 1999). Outside HE however, hemispheric climates remain synchronized by global teleconnection (Broecker 1998).

5. DO-cycle

5.1 Phenomenology

The cooling phase of H-cycle is populated by millennial-scale DO-cycles to form bundled Bond cycle (Dansgaard et al. 1993; Bond et al. 1993). Its hierarchical structure is intriguing: DO-cycles emerge only after post-HE warming, and then both their stades/interstades follow the H-cooling trend. The stades are accompanied by IRD (Bond et al. 1997; van Kreveld et al. 2000), suggesting their origin in ice calving, which endows abruptness to the millennial-scale DO-cycle.

Despite this common origin in ice calving, DO-cycle differs from H-cycle in important respects: first, the freshwater flux is considerably smaller (Yokoyama and Esat 2011), suggesting calving only of the marginal ice (Sect. 2); second, while SAT range remains large, SST and MOC signals are further muted and no hemispheric linkage can be discerned (Bond et al. 1995; Charles et al. 1996; Elliot et al. 2002); third, unlike saw-toothed H-cycle, DO-cycle is more symmetric with comparable millennial duration for both stades and interstades (Alley 1998).

Perhaps the most significant observation of DO-cycle is its prevalence in Holocene even in the absence of large ice sheet and H-cycle (Bond et al. 1997). Yet, the Holocene DO-cycle is still accompanied by IRD and retains similar time signature as its glacial counterpart, suggesting their common genesis (Bond et al. 1997). Without sea ice covering the subpolar ocean, the SAT range of Holocene DO-cycle is much reduced, and SST and MOC signals are indistinct (Grootes and Stuiver 1997), which certainly are unrelated to mode change; the common genesis of the Holocene and glacial DO-cycle thus further degrades the latter's interpretation as involving mode change.

5.2 Genesis

We have posited in Sect. 2 that DO-cycle has its origin in the periodic calving of the marginal ice of the ablation zone. Since during glacial time, there can be ablation only by the post-H warmth, the glacial DO-cycle thus is preconditioned on H-events and anchored on the cooling phase of the H-cycle. The genesis of the DO-cycle is illustrated in the phase space in Fig. 7, which thus is enclosed within the H-cycle marked by the thin outer line. Following the same convention as the H-cycle, the DO-cycle goes through numbered states with solid and dashed arrows indicating fast (decadal) ocean response and slow (millennial) MEP adjustment, respectively, and its time series is plotted in Fig. 8, for which we have assumed square-wave freshwater flux of 2 ky period (shaded columns) and dark shades symbolize the sea-ice cover.

https://doi.org/10.5194/egusphere-2022-208
Preprint. Discussion started: 11 May 2022

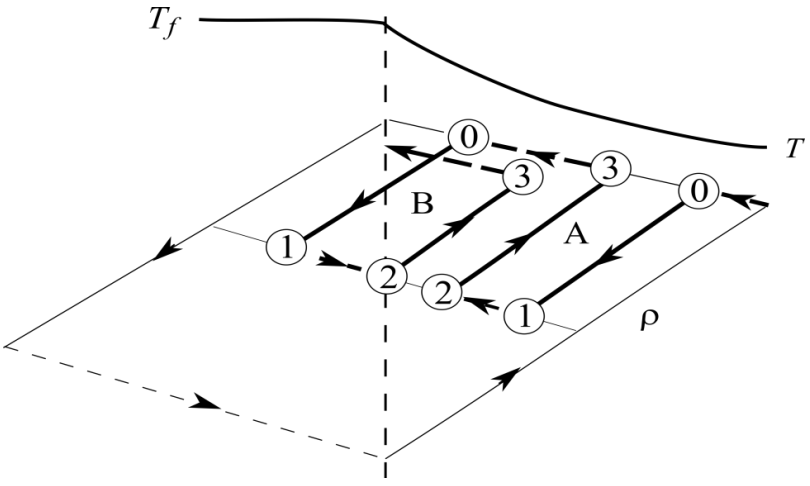

Figure 7: Same as Fig. 5, but for DO-cycles anchored on the cooling phase of H-cycle (thin lines). Type-A's stade remains above the freezing point while type-B's has reached the freezing point to resemble a mini-H-cycle.

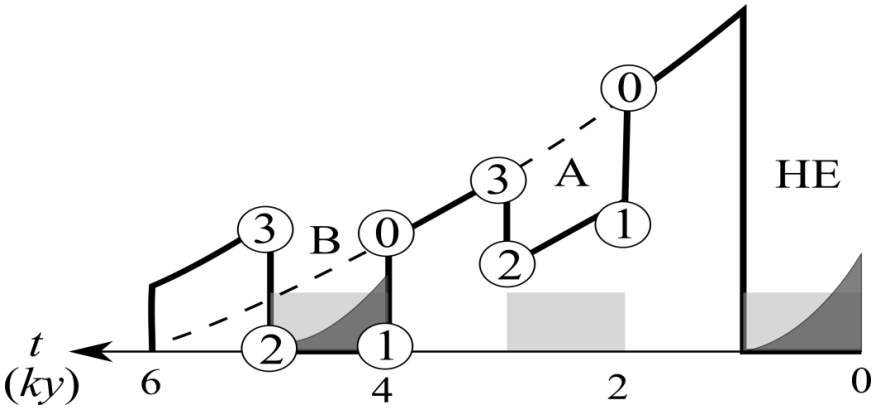

Figure 8: A schematic of a preceding HE and DO-cycles in the time domain corresponding to that of Fig. 7. Light and dark shades indicate freshwater fluxes (a square-wave of 2 ky period) and sea-ice cover. Type B's stade has reached freezing-point to cause formation of the sea-ice and a greater rebound of the ensuing interstade, but otherwise DO-cycles trend as the H-cooling curve to exhibit the hierarchical Bond cycle.

https://doi.org/10.5194/egusphere-2022-208
Preprint. Discussion started: 11 May 2022

Unlike H-cycle, we need to distinguish two types of DO cycle, designated as type-A and B in the figures. For type-A, its stade remains above the freezing point hence unobstructed in its trending of the H-cooling, so the ensuing interstade simply returns to the H-cooling curve in the time plot. For type-B however, its stade has reached the freezing point to cause formation of sea ice, just like the H-cycle, so the ensuing interstade would protrude above the cooling curve, resembling a miniature post-H warming. Despite the protrusion, both stades/interstades trend as H-cooling to exhibit hierarchical structure of the Bond cycle, as depicted in Alley (1998, Fig. 1).

While timing signature of the DO-cycle is controlled by internal ice dynamics, its initial trigger is due to the post-HE warmth whose timing thus is related to vertical advection associated with surface melt. As a cursory estimate, a summer melt rate of 2 $m\ y^{-1}$ (Oerlemans 1991) would yield vertical- and annual-averaged vertical velocity of O (0.5 $m\ y^{-1}$) to render an advective timescale of O (1 ky) hence it need not be differentiated from the creep duration.

5.3 Synthesis

Since DO-cycle is accompanied by IRD (Bond et al. 1997), we posit that it is originated in ice calving, just like HE except the thermal switch lies under the ablation zone to calve the marginal ice. This origin avails the DO-cycle with step-like freshwater flux of millennial duration --- its defining characteristics in common with H-cycle; but differing from the latter, the glacial DO-cycle commences only after the post-HE warmth has set up the ablation zone to activate its thermal switch, the reason that the glacial DO-cycle is encased within H-cycle to form the hierarchical Bond cycle. In the interglacial, on the other hand, the ablation zone is already in existence around Greenland ice sheet (Oerlemans 1991), so DO-cycle would be self-sustaining and retain the same time signature as its glacial counterpart. This commonality thus stems from ice dynamics of the ablation zone, not the large ice sheet whose absence in Holocene has led Bond et al. (1997) to conjecture (unknown) climate origin of the DO-cycle.

The large SAT signal of the glacial DO-cycle has been widely interpreted as indicative of ocean mode change (Broecker et al. 1990), which however may simply reflect the vast sea-ice cover during DO-stades that strongly cools the winter air (Denton et al. 2005; Li et al. 2010) whereas the SST signal remains short of mode change. Since there is little sea ice in the interglacial, the SAT signal of the Holocene DO-cycle is much reduced, and the SST variation is further muted and obviously is unrelated to mode change; its common genesis with the glacial DO-cycle would further militate against the latter's interpretation as involving mode change.

Besides the mode change (Ganopolski and Rahmstorf 2001) critiqued above, the DO-cycle has also been modelled as damped oscillation when the ocean is perturbed by freshwater forcing or noise (Sakai and Peltier 1999; Schulz and Paul 2002). The modelled period however depends critically on the strength of the perturbation, which is difficult to reconcile with the comparable time signature of Holocene and glacial DO-cycles: not only is there no anomalous freshwater flux in the interglacial, the HE-induced freshwater flux has already ceased before the onset of glacial DO-cycle for which the freshwater flux is its manifested cyclic signal, not an external

https://doi.org/10.5194/egusphere-2022-208
Preprint. Discussion started: 11 May 2022

stimulus. In our interpretation, the timing signature of DO-cycle is deterministic and set by the ice dynamics of the ablation zone, and the ocean role is relegated to setting-up the ablation zone in enabling the DO-cycle.

6. Deglaciation

6.1 Phenomenology

The most dramatic abrupt change occurred during last deglaciation, which is preceded by H1 and derailed by a temporary return to deep freeze in YD (Alley and Clark 1999). Multiple freshwater fluxes are discerned, which are accompanied by IRD and retain the millennial spacing of DO-cycles (Keigwin et al. 1991, Fig. 6; Bond et al. 1997, Fig. 6), suggesting their common origin in the periodic calving of the ice sheet. In addition, there are two massive meltwater pulses (MWP-1A and 1B) derived from meltback of LIS by the interglacial warmth (Fairbanks 1989).

The meltwater is rerouted from Mississippi to St. Lawrence rivers when LIS has sufficiently re-treated, which may reinforce the calving-induced freshwater flux to cause YD (Broecker et al. 1988; Teller 1990; Marchitto and Wei, 1995). The coldness of YD however halts MWP-1A as seen in the glacial readvance (Broecker et al. 1988), resulting in only small overlap between the two (Lehman and Keigwin 1992). Since LIS has largely disintegrated during the Preboreal, MWP-1B causes only moderate cooling marking the 8.2 ka event (Alley et al. 1997). As an added puzzle, the YD-like climate reversal did not occur during penultimate deglaciation (Carl-son 2008).

As freshening and cooling have opposite effects on marine δ^{18}O, their relative importance would muddle the interpretation of this data (Keigwin et al. 1991). Both H1 and YD however manifest strongly in the ice-core δ^{18}O because of the extremely cold winter air (Denton et al. 2005), and the shutdown of MOC during these events has caused Antarctic warming and rising global pCO_2 (Broecker 1998; Shakun et al. 2012), which thus precede the northern climate rebound.

6.2 Genesis

We illustrate the deglaciation in the phase-space diagram in Fig. 9 and its time progression in Fig. 10. Since the freshwater flux is derived from the same source as that of DO-cycle, it is set as a square wave of 2 ky period (light-shaded), which turns out to produce deglaciation events like the observed ones hence as labelled. We have drawn two meltwater pulses caused by the in-terglacial warmth based on observation and the timing constraint noted above. Since the summer insolation has risen from the deep glacial, we set $q = .8$ (that is, annul absorbed solar flux is 80 Wm^{-2} below the global mean) so the temperature (deficit) and density (surplus) curves are low-ered from those of Fig. 5 and for simplicity we set the same freshwater flux of .1 Sv.

https://doi.org/10.5194/egusphere-2022-208
Preprint. Discussion started: 11 May 2022

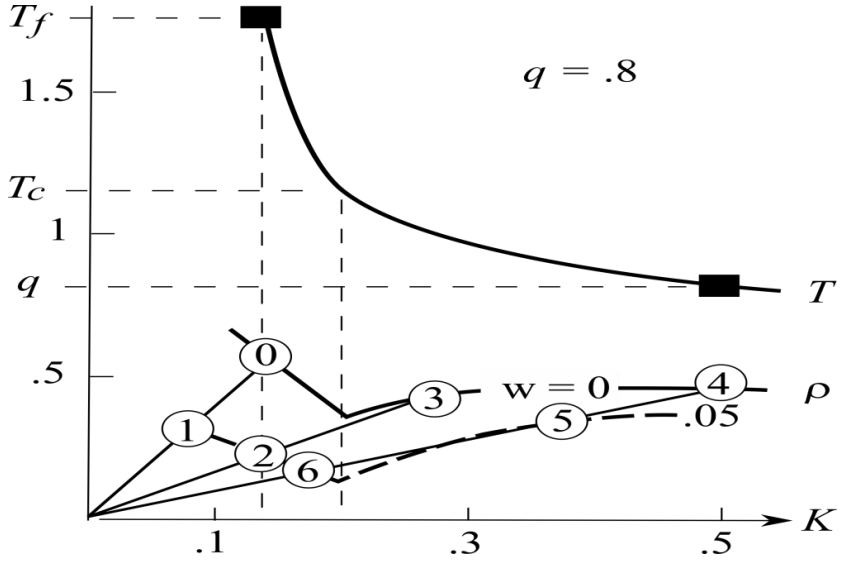

Figure 9: Same as Fig. 5 but for $q = .8$, depicting deglaciation sequence.

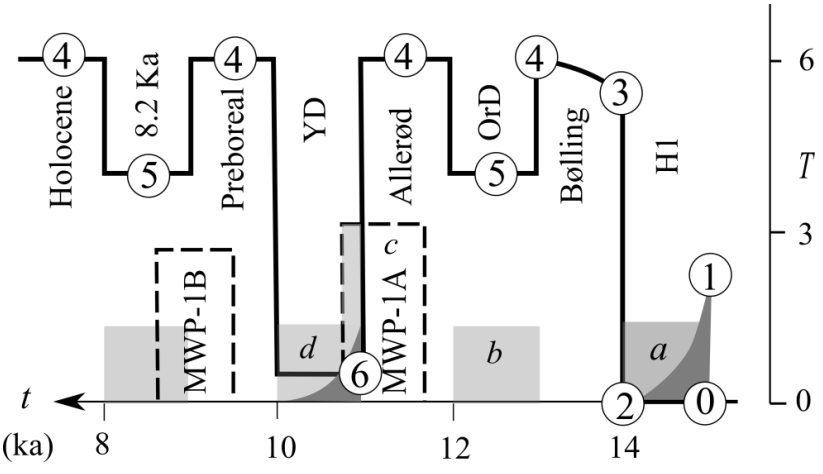

Figure 10: Time progression of the deglaciation shown in Fig. 9 with corresponding observed events labelled. Light shades are freshwater fluxes of a square wave of 2-ky period with letters *a-d* corresponding to meltwater events identified in Keigwin et al. (1991). Dark shades indicate sea-ice covers.

https://doi.org/10.5194/egusphere-2022-208
Preprint. Discussion started: 11 May 2022

The climate signal begins with the glacial MEP (State 0) and runs through numbered states. The transition from State 0 to 1 to 2 are like the H-cycle, but because of the rising summer insolation, the MOC line flattened by HE no longer intersects the density curve in the cold branch, so the climate would vault into the warm branch (State 3), marking the initial deglaciation. Equating the post-HE temperature Eq. (15) with the convective bound Eq. (5), we derive the criterion for the deglaciation

$$\frac{w}{q_e} \geq 1 - \left(\frac{T_c}{T_f}\right)^2 . \tag{17}$$

The rhs depends on global-mean temperature and convective flux, which set the long-term super-orbital condition; the lhs on the other hand depends on both freshwater perturbation and orbital forcing: a greater freshwater flux would cause deglaciation even with lower summer insolation. With the standard parameters listed in Appendix, the rhs is .59; and for meltwater flux of .1 Sv, the deglaciation would occur when annual absorbed SW flux reaches about 81 Wm^{-2} below the global mean, consistent with that seen in Fig. 9. In comparison, the orbital forcing needs to be 8 Wm^{-2} higher without HE; but since such insolation increase is nonetheless attained in about a millennium, HE may not delay (McCabe and Clark 1998) --- and possibly even hasten --- the deglaciation. On the other hand, since recurring time of HE is shorter than the half precession cycle (10 ky), it always punctuates the deglaciation, as is the observed case (McManus et at. 1999, Fig. 4).

Following the initial deglaciation, State 3 would propel to State 4 (the interglacial MEP), a transition spanning the Bølling interstadial. The warmth would elevate the snowline to cause calving of the marginal ice after a millennium, just like DO-cycle, and the resulting freshwater flux would cool State 4 to 5 marking Older Dryas (OrD), which however remains an interglacial. The continuing Allerød warmth (State 4) would melt back LIS to generate massive MWP-1A, but differing from the northern calving, the meltwater does not perturb the climate until the ice margin has sufficiently retreated to allow the meltwater to be rerouted to the Hudson Bay. And then it would reinforce the northern calving by further lowering the density curve (not drawn) to vault State 4 to 6 marking the YD. Unlike calving paced by internal ice dynamics, the meltback would be halted by the cold YD, as seen in the glacial readvance. Here for simplicity, we have neglected the lesser pivot of the MOC line during YD because the small density surplus has in effect rigidified the MOC line (Ou 2018), so the termination of the millennial YD would rebound the climate from State 6 to 4, the latter corresponding to the Preboreal. The recurring ice calving after a millennium causes the 8.2 ka cooling event (State 5), which is analogous to OrD, and since LIS has largely disintegrated during Preboreal, MWP-1B is insufficient to cause the glacial flip. After the 8.2 ka event, the climate returns to State 4 corresponding to the Holocene.

6.3 Synthesis

https://doi.org/10.5194/egusphere-2022-208
Preprint. Discussion started: 11 May 2022

The ultimate driver of deglaciation is the rising summer insolation during increasing eccentricity (Ou 2022b), the suborbital deglaciation events however can be explained by the interplay of three distinct sources of the freshwater perturbation. The first is calving of the inland ice that triggers H1, whose post-event warming would vault the glacial into interglacial. The latter sets up an ablation zone to enable the second source: a periodic calving of the marginal ice, just like that drives the millennial DO-cycle, whose stades can be identified with OrD, YD and 8.2 ka event. The glacial flip of YD however requires a third source: the rerouting of the meltwater generated by meltback of LIS (MWP-1A). Since rerouting occurs only after LIS has sufficiently retreated, and the cold YD would halt the meltback, there can only be small overlap between YD and MWP-1A (Duplessy et al. 1992; Lehman and Keigwin 1992). This timing mismatch has raised question about their causal linkage (Fairbanks 1989), which however is resolved here by the combined effect of second and third freshwater sources. Since YD involves happenstance of rerouting and remnant of meltwater, such dramatic climate reversal is not inevitable and indeed did not occur during MWP-1B or penultimate deglaciation.

As YD is accompanied by strong freshening and cooling, they could cancel each other to leave little imprint on the marine δ^{18}O data, H1 however is initiated from a glacial state, so freshening dominates to register in this data (Duplessy et al. 1992, Fig. 1). Both YD and H1 however manifest strongly in the ice-core δ^{18}O because of the extremely cold winter air insulated from ocean heat by extensive sea ice (Denton et al. 2005). The first three freshwater fluxes and MWP-1A shown in Fig. 10 can be identified with the four meltwater events discerned in Keigwin et al. (1991, their Fig. 6), and our model offers a plausible interpretation of the diverse marine δ^{18}O signal: events *a* and *d* are associated with strong cooling (as symbolized by the shaded sea-ice cover) to cause maxima in the data, but events *b* and *c* involve little cooling hence dominated by freshening to yield minima.

While YD is triggered by freshwater flux, its freshening is due primarily to the MOC shutdown (Duplessy et al. 1992), which would sequester the southern heat to cause Antarctic warming (Broecker 1998; Stocker 2000). As such, the latter and the accompanying rising pCO_2 precede the northern climate rebound (Shakun et al. 2012), which however are not causal since the northern deglaciation is already underway and only temporarily reversed by YD on account of the internal ice dynamics. The termination of YD is accompanied by doubling of accumulation, which has been attributed to atmospheric circulation change (Alley et al. 1993) but it may simply reflect the more moist interglacial air, just like that induced by global warming.

That the enhanced moisture transport by global warming may shut down MOC, like the triggering of YD, is a topic widely examined in the past (Manabe and Stouffer 1999; Rahmstorf et al. 2005; Ou 2018). Model intercomparisons however show considerable uncertainty in the freshwater threshold, which can be assessed from our model. As the northern summer insolation has dimmed since about 10 ka (Alley and Clark 1999), it would raise the freshwater threshold based on our phase-space diagram (comparing Figs. 5 and 9), but even the lower threshold and the

https://doi.org/10.5194/egusphere-2022-208
Preprint. Discussion started: 11 May 2022

massive MWP-1B at 8 ka have caused only moderate cooling, we envisage therefore little prospect of a glacial flip; the next glaciation is likely gradual, evolving over millennial timescale (Ou 2022b), just like previous ones.

7. Conclusions

We integrate our ice-sheet and climate models to address abrupt climate changes pertaining to H- and DO-cycles as well as the last deglaciation punctuated by YD. Since they are all accompanied by IRD, we posit a common source of freshwater perturbation from periodic calving of the ice sheet due to thermal switch at its bed. We however distinguish two different sources of the thermal switches: one from trapping of the geothermal heat, which would calve inland ice that causes HE; the other from surface melt of the ablation zone, which would calve the marginal ice to drive the DO-cycle. Since ablation zone can be set up in the glacial time only by post-HE warmth, the glacial DO-cycle is preconditioned on HE to form the Bond cycle; in contrast, the ablation is already operative during interglacial, so there is self-sustaining Holocene DO-cycle even in the absence of large ice sheet or HE. In addition to the thermal switch paced by internal ice dynamics, the meltback of LIS by interglacial warmth would generate massive meltwater pulses and if the meltwater is rerouted to the Hudson Bay, it may augment calving-induced freshwater flux to cause YD, a dramatic reversal of the deglaciation.

Since the thermal switch operates on extremely short (years) subglacial hydrological timescale, the resulting freshwater flux is step-like, and then ocean responds to this flux on decadal timescale, they together would endow abruptness to these climate signals, which thus need not involve ocean mode change, as commonly assumed. Since recuring calving is constrained by mass balance, it is naturally availed millennial timescale. This timescale however is not inherent to the ocean and may emerge in numerical simulations only under tenuous external condition or stimulus, which is at odds with robust time signature of the observed signals.

In addition to the common origin in the ice calving depicted in our ice-sheet model (Ou 2022a), our climate model (Ou 2018) has underscored a key process in the ocean response. Recognizing that MOC is subjected to random eddy shedding across the subtropical front, we apply probability law of the NT to deduce that it would be propelled on millennial timescale toward MEP. As a direct consequence of this MEP adjustment, termination of HE is characterized by a sudden warming to be followed by gradual cooling to exhibit saw-toothed H-cycle, and then the cooling trend would anchor DO-cycles to form the hierarchical Bond cycle. The YD, just like other freshwater perturbation, is paced by the internal ice dynamics but it requires reinforcement from the rerouted meltwater to cause the glacial flip. As it involves happenstance of rerouting, such dramatic climate reversal did not occur during the penultimate deglaciation.

By incorporating the calving origin of the freshwater perturbation and the MEP adjustment of the ocean, our theory has provided an integral account of abrupt climate changes. There is no need to invoke disparate or extraneous physics in explaining their diverse features, as seen in our syn-

https://doi.org/10.5194/egusphere-2022-208
Preprint. Discussion started: 11 May 2022

thesis of previous works. The robustness of deduced features and their resemblance of the observed ones suggest that our theory might have isolated the governing physics of abrupt climate changes.

Appendix

a_s	Aspect ratio of surging ice
$\dot{a}$	Accumulation ($= .1\ m\ a^{-1}$)
$C_{p,o}$	Specific heat of ocean ($= 4.2 \times 10^3\ J\ Kg^{-1}\ {}^0C^{-1}$)
g	Gravitation acceleration ($= 9.8\ m\ s^{-2}$)
$\dot{g}$	Geothermal flux ($= 6 \times 10^{-2}\ Wm^{-2}$)
h_s	Ice height at surge termination
$[h]$	ELA for DO-cycle ($= .5\ km$)
K	MOC mass flux
$[K]$	Scale of K ($= \alpha^* l(2\rho_o C_{p,o})^{-1} = 6\ m^2 s^{-1}$)
l	Latitudinal span of subpolar ocean ($= 4 \times 10^3\ km$)
L	North Atlantic basin width ($= 6 \times 10^3\ km$)
q	Cold-box deficit of absorbed solar flux
q_e	Excess forcing over warm-transition threshold
$[q]$	Scale of q ($= 100\ Wm^{-2}$)
$\bar{q}_c$	Global convective flux
S	Cold-box salinity deficit
S_0	Reference salinity (=35)
$[S]$	Scale of S ($= \alpha[T]/\beta$=1)
t_{ratio}	ratio of surge/creep duration
$[t]$	Timescale for DO-cycle ($\equiv [h]/\dot{a} =$ 5 ky)
T	Cold-box SST deficit
T_c	Convective-bound temperature
T_f	Freezing-point temperature
$[T]$	Scale of T($= [q]/\ \alpha^* = 8\ {}^0$C)
$\bar{T}$	Global-mean SST (=14 ^{0}C)
ΔT	Temperature range of H-cycle
w	Freshwater flux
$[w]$	Scale of w ($= 2[K][S]/S_0 = .34\ m^2 s^{-1}$)
α	Thermal expansion coefficient ($= 10^{-4}\ {}^0C^{-1}$)
α_h	Heating parameter (=.48)
α^*	Air-sea transfer coefficient ($= 12.5\ Wm^{-2}\ {}^0C^{-1}$, Ou 2018)
β	Saline contraction coefficient ($= 8 \times 10^{-4}$)
ρ	Cold-box density surplus
$[\rho]$	Scale of ρ ($= \rho_o \alpha[T] = .8\ Kg\ m^{-3}$)
ρ_i	Ice density ($= .92 \times 10^3\ Kg\ m^{-3}$)
ρ_o	Reference ocean density ($= 10^3\ Kg\ m^{-3}$)

https://doi.org/10.5194/egusphere-2022-208
Preprint. Discussion started: 11 May 2022

μ Moisture parameter (= 0.3)

References

Alley RB (1998) Icing the north Atlantic. Nature 392(6674):335-7 https://doi.org/10.1038/32781

Alley RB, Clark PU (1999) The deglaciation of the northern hemisphere: a global perspective. Annu Rev Earth Planet Sci 27(1):149-82 https://doi.org/10.1146/annurev.earth.27.1.149

Alley RB, Marotzke J, Nordhaus WD, Overpeck JT, Peteet DM, Pielke RA, Pierrehumbert RT, Rhines PB, Stocker TF, Talley LD, Wallace JM (2003) Abrupt climate change. Science 299(5615):2005-10 https://doi.org/10.1126/science.1081056

Alley RB, Mayewski PA, Sowers T, Stuiver M, Taylor KC, Clark PU (1997) Holocene climatic instability: A prominent, widespread event 8200 years ago. Geol 25:483–6 https://doi.org/10.1130/0091-7613(1997)025<0483:hciapw>2.3.co;2

Alley RB, Meese DA, Shuman CA, Gow AJ, Taylor KC, Grootes PM, White JWC, Ram M, Waddington ED, Mayewski PA, Zielinski GA (1993) Abrupt increase in snow accumulation at the end of the Younger Dryas event. Nature 362:527-529 https://doi.org/10.1038/362527a0

Auer SJ (1987) Five-year climatological survey of the Gulf Stream system and its associated rings. J Geophys Res 92:11709–26

Bard E (2002) Climate shock-Abrupt changes over millenial time scales. Phys Today 55(12):32-8 https://doi.org/10.1063/1.1537910

Bond G, Broecker W, Johnsen S, McManus J, Labeyrie L, Jouzel J, Bonani G (1993) Correlations between climate records from North Atlantic sediments and Greenland ice. Nature 365(6442):143-7 https://doi.org/10.1038/365143a0

Bond G, Heinrich H, Broecker W, Labeyrie L, McManus J, Andrews J, Huon S, Jantschik R, Clasen S, Simet C, Tedesco K (1992) Evidence for massive discharges of icebergs into the North Atlantic ocean during the last glacial period. Nature 360(6401):245-9 https://doi.org/10.1038/360245a0

Bond GC, Lotti R (1995) Iceberg discharges into the North Atlantic on millennial time scales during the last glaciation. Science 267(5200):1005-10 https://doi.org/10.1126/science.267.5200.1005

https://doi.org/10.5194/egusphere-2022-208
Preprint. Discussion started: 11 May 2022

619 Bond G, Showers W, Cheseby M, Lotti R, Almasi P, DeMenocal P, Priore P, Cullen H, Hajdas I,
620 Bonani G (1997) A pervasive millennial-scale cycle in North Atlantic Holocene and gla-
621 cial climates. Science 278(5341):1257-66 https://doi.org/10.1126/science.278.5341.1257

622 Brinkerhoff DJ, Johnson JV (2015) Dynamics of thermally induced ice streams simulated with a
623 higher-order flow model. J Geophys Res Earth Surf 120(F9):1743–70
624 https://doi.org/10.1002/2015jf003499

625 Broecker WS (1994) Massive iceberg discharges as triggers for global climate change. Nature
626 372:421-4 https://doi.org/10.1038/372421a0

627 Broecker WS (1998) Paleocean circulation during the last deglaciation: A bipolar seesaw?
628 Paleoceanogr 13:119–21 https://doi.org/10.1029/97pa03707

629 Broecker WS, Andree M, Wolfli W, Oeschger H, Bonani G, Kennett J, Peteet D (1988) The
630 chronology of the last deglaciation: Implications to the cause of the Younger Dryas event.
631 Paleoceanogr Paleoclimatol 3(1):1-9 https://doi.org/10.1029/pa003i001p00001

632 Broecker WS, Bond G, Klas M, Bonani G, Wolfli W (1990) A salt oscillator in the glacial Atlan-
633 tic? 1. The concept. Paleoceanogr 5(4):469-77 https://doi.org/10.1029/pa005i004p00469

634 Calov R, Ganopolski A, Petoukhov V, Claussen M, Greve R (2002) Large-scale instabilities of
635 the Laurentide ice sheet simulated in a fully coupled climate-system model. Geophys Res
636 Lett 29(24):2216 https://doi.org/10.1029/2002GL016078

637 Carlson A (2008) Why there was not a Younger Dryas-like event during the Penultimate Degla-
638 ciation? Quat Sci Rev 27(9–10):882–7 https://doi.org/10.1016/j.quascirev.2008.02.004

639 Chappell J (2002) Sea level changes forced ice breakouts in the Last Glacial cycle: new results
640 from coral terraces. Quat Sci Rev 21(10):1229–40 https://doi.org/10.1016/s0277-
641 3791(01)00141-x

642 Charles CD, Lynch-Stieglitz J, Ninnemann US, Fairbanks RG (1996) Climate connections be-
643 tween the hemisphere revealed by deep sea sediment core/ice core correlations. Earth
644 Planet Sci Lett 142(1-2):19-27 https://doi.org/10.1016/0012-821x(96)00083-0

645 Clark PU (1992) Surface form of the southern Laurentide Ice Sheet and its implications to ice
646 sheet dynamics. Geol Soc Am Bull 104:595-605 https://doi.org/10.1130/0016-
647 7606(1992)104<0595:sfotsl>2.3.co;2

648 Clark PU, Alley RB, Pollard D (1999) Northern Hemisphere ice sheet influences on global cli-
649 mate change. Science 286:1104–11 https://doi.org/10.1126/science.286.5442.1104

https://doi.org/10.5194/egusphere-2022-208
Preprint. Discussion started: 11 May 2022

650 Clark PU, Pisias NG, Stocker TF, Weaver AJ (2002) The role of the thermohaline circulation in
651 abrupt climate change. Nature 415:863-9 https://doi.org/10.1038/415863a

652 Crooks GE (1999) Entropy production fluctuation theorem and the nonequilibrium work relation
653 for free energy differences. Phys Rev E 60(3):2721–6

654 Dansgaard W, Johnsen SJ, Clausen HB, Dahl-Jensen D, Gundestrup NS, Hammer CU, Hvidberg
655 CS, Steffensen JP, Sveinbjörnsdottir AE, Jouzel J, Bond G (1993) Evidence for general
656 instability of past climate from a 250-kyr ice-core record. Nature 364(6434):218-20
657 https://doi.org/10.1038/364218a0

658 Denton GH, Alley RB, Comer GC, Broecker WS (2005) The role of seasonality in abrupt cli-
659 mate change. Quat Sci Rev 24(10-11):1159-82 https://doi.org/10.1016/j.quasci-
660 rev.2004.12.002

661 Duplessy JC, Bard E, Arnold M, Shackleton NJ, Duprat J, Labeyrie L (1991) How fast did the
662 ocean-atmosphere system run during the last deglaciation? Earth Planet Sci Lett 103(1-
663 4):27-40 https://doi.org/10.1016/0012-821x(91)90147-a

664 Duplessy JC, Labeyrie L, Arnold M, Paterne M, Duprat J, van Weering TC (1992) Changes in
665 surface salinity of the North Atlantic Ocean during the last deglaciation. Nature
666 358(6386):485-8

667 Elliot M, Labeyrie L, Duplessy JC (2002) Changes in North Atlantic deep-water formation asso-
668 ciated with the Dansgaard–Oeschger temperature oscillations (60–10 ka). Quat Sci Rev
669 21(10):1153-65 https://doi.org/10.1016/s0277-3791(01)00137-8

670 Fairbanks RG (1989) A 17,000-year glacio-eustatic sea level record: Influence of glacial melting
671 rates on the Younger Dryas event and deep-ocean circulation. Nature, 342:637-42

672 Fricker HA, Scambos T, Bindschadler R, Padman L (2007) An active subglacial water system in
673 West Antarctica mapped from space. Science 315(5818):1544–8 https://doi.org/10.1126/
674 science.1136897

675 Ganopolski A, Rahmstorf S (2001) Rapid changes of glacial climate simulated in a coupled cli-
676 mate model. Nature 409:153-8

677 Grootes PM, Stuiver M (1997) Oxygen 18/16 variability in Greenland snow and ice with 103- to
678 105-year time resolution. J Geophys Res 102:26455-70

679 Grousset FE, Labeyrie L, Sinko JA, Cremer M, Bond G, Duprat J, Cortijo E, Huon S (1993) Pat-
680 terns of ice-rafted detritus in the glacial North Atlantic (40–55° N). Paleoceanogr
681 8(2):175-92 https://doi.org/10.1029/92pa02923

https://doi.org/10.5194/egusphere-2022-208
Preprint. Discussion started: 11 May 2022

682 Heinrich H (1988) Origin and consequences of cyclic ice rafting in the northeast Atlantic Ocean
683 during the past 130,000 years. Quat Res 29:142-52 https://doi.org/10.1016/0033-
684 5894(88)90057-9

685 Hemming SR (2004) Heinrich events: massive late Pleistocene detritus layers of the North At-
686 lantic and their global climate imprint. Rev Geophys 42(1):RG1005,1-43
687 https://doi.org/10.1029/2003RG000128

688 Henry LG, McManus JF, Curry WB, Roberts NL, Piotrowski AM, Keigwin LD (2016) North
689 Atlantic ocean circulation and abrupt climate change during the last glaciation. Science
690 353(6298):470-4 https://doi.org/10.1126/science.aaf5529

691 Hooke RL (1977) Basal temperatures in polar ice sheets: a qualitative review. Quat Res 7(1):1-
692 13 https://doi.org/10.1016/0033-5894(77)90011-4

693 Keigwin LD, Jones GA, Lehman SJ, Boyle EA (1991) Deglacial meltwater discharge, North At-
694 lantic deep circulation, and abrupt climate change. J Geophys Res Oceans 96(C9):16811-
695 26 https://doi.org/10.1029/91jc01624

696 Kucera M, Weinelt M, Kiefer T, Pflaumann U, Hayes A, Weinelt M, Chen MT, Mix AC, Bar-
697 rows TT, Cortijo E, Duprat J (2005) Reconstruction of sea-surface temperatures from as-
698 semblages of planktonic foraminifera: multi-technique approach based on geographically
699 constrained calibration data sets and its application to glacial Atlantic and Pacific Oceans.
700 Quat Sci Rev 24(7-9):951-98 https://doi.org/10.1016/j.quascirev.2004.07.014

701 Lehman SJ, Keigwin JD (1992) Sudden changes in North Atlantic circulation during the last de-
702 glaciation. Nature 356:757–62 https://doi.org/10.1038/356757a0

703 Li C, Battisti DS, Bitz CM (2010) Can North Atlantic sea ice anomalies account for Dansgaard–
704 Oeschger climate signals? J Clim 23(20):5457-75
705 https://doi.org/10.1175/2010JCLI3409.1

706 Lozier MS (2010) Deconstructing the conveyer belt. Science 328(5985):1507-11
707 https://doi.org/10.1126/science.1189250

708 MacAyeal DR (1993) Binge/purge oscillations of the Laurentide ice sheet as a cause of the North
709 Atlantic's Heinrich events. Paleoceanogr 8(6):775-84 https://doi.org/10.1029/93pa02200

710 Manabe S, Stouffer RJ (1988) Two stable equilibria of a coupled ocean-atmosphere model. J
711 Clim 1:841-66 https://doi.org/10.1175/1520-0442(1988)001<0841:tseoac>2.0.co;2

712 Manabe S, Stouffer R (1999) The role of thermohaline circulation in climate. Tellus A 51(1):91-
713 109 https://doi.org/10.1034/j.1600-0870.1999.t01-1-00008.x

https://doi.org/10.5194/egusphere-2022-208
Preprint. Discussion started: 11 May 2022

714 Marchitto TM, Wei KY (1995) History of Laurentide meltwater flow to the Gulf of Mexico dur-
715 ing the last deglaciation, as revealed by reworked calcareous nannofossils. Geology
716 23(9):779-82

717 McCabe AM, Clark PU (1998) Ice-sheet variability around the North Atlantic Ocean during the
718 last deglaciation. Nature 392(6674):373-7 https://doi.org/10.1038/32866

719 McManus JF, Oppo DW, Cullen JL (1999) A 0.5-million-year record of millennial-scale climate
720 variability in the North Atlantic. Science 283(5404):971-5 https://doi.org/10.1126/sci-
721 ence.283.5404.971

722 Oerlemans J (1991) The mass balance of the Greenland ice sheet: sensitivity to climate change as
723 revealed by energy-balance modelling. Holocene 1(1):40-8
724 https://doi.org/10.1177/095968369100100106

725 Ou H-W (2018) Thermohaline circulation: a missing equation and its climate change implica-
726 tions. Clim Dyn 50:641-53 https://doi.org/10.1007/s00382-017-3632-y

727 Ou H-W (2022a) A theory of glacier dynamics and instabilities Part 1: Topographically confined
728 glaciers. J Glaciol 68(267):1–12 https://doi.org/ 10.1017/jog.2021.20

729 Ou H-W (2022b) A theory of glacial cycles: Resolving Pleistocene puzzles. Under review at
730 Paleoceanogr https://www.essoar.org/doi/10.1002/essoar.10509978.1

731 Paillard D (1995) The hierarchical structure of glacial climatic oscillations: Interactions between
732 ice-sheet dynamics and climate. Clim Dyn 11:162–77
733 https://doi.org/10.1007/s003820050068

734 Rahmstorf S, Crucifix M, Ganopolski A, Goosse M, Kamenkovich I, Knutti R, Lohmann G,
735 Marsh R, Mysak LA, Wang Z, Weaver AJ (2005) Thermohaline circulation hysteresis: A
736 model intercomparison. Geophys Res Lett 32(23) L23605, doi:10.1029/2005GL023655

737 Sakai K, Peltier WR (1999) A dynamical system model of the Dansgaard–Oeschger oscillations
738 and the origin of the Bond cycle. J Clim 12:2238–55 https://doi.org/10.1175/1520-
739 0442(1999)012<2238:adsmot>2.0.co;2

740 Schulz M, Paul A (2002) Holocene climate variability on centennial-to-millennial time scales: 1.
741 Climate records from the North-Atlantic realm. In: Climate development and history of
742 the North Atlantic realm (p 41-54). Springer, Berlin, Heidelberg.

743 Shakun JD, Clark PU, He F, Marcott SA, Mix AC, Liu Z, Otto-Bliesner B, Schmittner A, Bard E
744 (2012) Global warming preceded by increasing carbon dioxide concentrations during the
745 last deglaciation. Nature 484(7392):49-54

https://doi.org/10.5194/egusphere-2022-208
Preprint. Discussion started: 11 May 2022

746 Stocker TF (2000) Past and future reorganization in the climate system. Quat Sci Rev 19:301-19
747 https://doi.org/10.1016/s0277-3791(99)00067-0

748 Stommel H (1961) Thermohaline convection with two stable regimes of flow. Tellus 13:224-30
749 https://doi.org/10.1111/j.2153-3490.1961.tb00079.x

750 Teller JT (1990) Meltwater and precipitation runoff to the North Atlantic, Arctic, and Gulf of
751 Mexico from the Laurentide ice sheet and adjacent regions during the Younger Dryas.
752 Paleoceanogr 5:897–905 https://doi.org/10.1029/pa005i006p00897

753 Tulaczyk S, Kamb WB, Engelhardt HF (2000) Basal mechanics of Ice Stream B, west Antarc-
754 tica: 2. Undrained plastic bed model. J Geophys Res 105(B1):483–94
755 https://doi.org/10.1029/1999jb900328

756 Van Kreveld S, Sarnthein M, Erlenkeuser H, Grootes P, Jung S, Nadeau MJ, Pflaumann U,
757 Voelker A (2000) Potential links between surging ice sheets, circulation changes, and the
758 Dansgaard-Oeschger cycles in the Irminger Sea, 60–18 kyr. Paleoceanogr 15(4):425-42
759 https://doi.org/10.1029/1999pa000464

760 Yokoyama Y, Esat TM (2011) Global climate and sea level: Enduring variability and rapid fluc-
761 tuations over the past 150,000 years. Oceanogr 24(2):54-69 https://doi.org/10.5670/
762 oceanog.2011.27